Cryogenically cooled 2.8 μm Er:YAP laser with watt-level output power

Cryogenically cooled 2.8-μm Er:YAP laser with watt-level output power

Enhao Li[1], Weichao Yao[2], Hiyori Uehara[1,2], Ryo Yasuhara[1,2,*]

[1]*The Graduate University for Advanced Studies, SOKENDAI, 322-6 Oroshi-cho, Toki 509-5292, Japan*
[2]*National Institute for Fusion Science, 322-6 Oroshi-cho, Toki 509-5292, Japan*

E-mail: *yasuhara@nifs.ac.jp*

We report the first watt-level, cryogenically cooled Er:YAP laser operating in the 3-μm spectral region. The spectroscopic properties of a 5 at.% Er:YAP crystal were studied at cooling temperatures ranging from 77–290 K. The fluorescence lifetime of the $^4I_{11/2}$ level associated with the 3-μm laser transition decreased with an increase in temperature; whereas, the lifetime of the $^4I_{13/2}$ level increased with an increase in temperature. Moreover, over 1 W of output power at 2798 nm was achieved from the liquid-nitrogen-cooled Er:YAP laser with a slope efficiency of 20%, and the limitations to higher output power were discussed.

Mid-infrared lasers emitting in the 3-μm wavelength region are a significant research area in the laser field, due to their significant applications in high-resolution water molecular dynamics [1] and directional remote sensing [2]. Additionally, high-power 3-μm lasers are ideally suited for pumping Fe^{2+}-doped lasers [3-5], Dy^{3+}-doped lasers [6], and nonlinear frequency conversion lasers [7] to extend spectral accessibility to a region with longer wavelengths. To date, laser diode (LD) pumped Er^{3+}-doped lasers demonstrate unique advantages among 3-μm lasers in terms of their compactness, power scaling capacity, and high wall-plug efficiency [8-12]. The Er:ZBLAN fiber laser, which delivers the highest output power among 3-μm Er lasers [12], is the most preferable for the power scaling of mid-infrared lasers. However, due to the low mechanical strength of ZBLAN soft glass and the property of water absorption on the fiber tips, Er:ZBLAN fibers are extremely difficult to handle. Therefore, Er-doped bulk lasers based on materials with low phonon energies, e.g., Er:YAP, Er:Y_2O_3, and Er:Lu_2O_3, are an alternative approach to the power scaling of 3-μm lasers. Various methods have been applied to study the power-scaling capacity of 3 μm Er solid-state lasers [8, 10, 13, 14].

Cryogenically cooled lasers are an advanced technique for the development of high-power lasers [15], given that the thermal properties of laser gain materials exhibit significant improvements at low temperatures. This feature is also attractive for 3-μm Er-doped solid-state lasers because thermal effects (the thermal lensing effect and thermally induced wavefront distortion) and the subsequent material damage are the primary limitations to their power scaling behaviors. However, the laser performance can be significantly improved at low temperatures. In 2010, a cryogenic sesquioxide Er:Y_2O_3 ceramic laser was reported by T. Sanamyan et.al., which generated an output power of 14 W and a slope efficiency of 26% at 2.7 μm [16]. In 2016, detailed spectroscopic properties of a cryogenic Er:Y_2O_3 ceramic were reported by the same group, and the output power of 24 W represents the highest output power reported from a 3-μm Er-doped solid-state laser [17]. The significant improvement in the output power demonstrates the potential of the cryogenic laser in the 3-μm mid-infrared wavelength region. As an alternative laser material for 3-μm lasers, Er:YAP crystal possesses low phonon energy (550 cm^{-1}) and excellent mechanical properties. The thermal shock resistance of YAP is significantly higher than that of a typical garnet host material such as YAG [8], thus indicating its potential for high-power laser operation. Significant progress was reported with respect to mid-infrared Er:YAP lasers operating at room temperature [8,14,18]. In 2018, the temperature-dependent spectroscopic properties of a low-doped Er:YAP crystal (1 at.% of Er^{3+}) were presented by R. Svejkar et. al., and the results revealed

higher output powers and slope efficiencies at cryogenic cooling temperatures than at room temperature [19]. However, the Er:YAP used in [19] was not optimized in terms of the doping concentration and crystal length; thus, the continuous wave (CW) output power was limited to 27 mW with a slope efficiency of only 3.5%. The spectroscopic properties of the highly doped Er:YAP crystal, in addition to its laser performance under cryogenic conditions, therefore require investigation for the further power scaling of the 3-μm lasers.

In this study, we aim to measure the spectroscopic properties of a highly doped Er:YAP crystal at the liquid-nitrogen cooling temperature, and study its laser performance to determine the limitations to the power scaling of a cryogenic Er:YAP laser. Watt-level output power was generated from a cryogenically cooled Er:YAP laser, which is approximately two orders of magnitude higher than the results reported in [19]. Additionally, this paper presents a discussion on the main factors limiting the laser power and efficiency.

The spectroscopic properties of the Er:YAP crystal, including its absorption spectrum and fluorescence lifetime, were first investigated to anticipate possible changes in the laser performance. Figure 1 shows the experimental setup used for the absorption spectrum measurement. An Er:YAP crystal (*b*-cut, space group: *Pbnm*; ordered from CRYTUR) with a doping concentration of 5 at.% was used. This 5 at.% doping concentration was chosen because it demonstrated excellent laser efficiency at room temperature in our previous study [8], meanwhile, it was a relatively low doping concentration among all reported 3-μm Er:YAP lasers operating at room temperature [20, 21], which implies a good balance between thermal effects and laser efficiency during lasing process. The crystal had a cross section of 2 mm × 5 mm and a length of 8 mm. It was wrapped in a piece of indium foil with a thickness of 0.1 mm, and mounted in a liquid-nitrogen-cooled copper heat sink. Two anti-reflective (AR) windows were used for the cryostat, and the pressure of the vacuum chamber was kept below 1.5 mTorr. A super-continuum (SC) light source (WhiteLase micro, FIANIUM) was used as the probe light, and an optical spectrum analyzer (Q8381A, ADVANTEST) with a resolution of 0.1 nm was used to measure the transmitted spectra of the SC light. The absorption spectra were derived by comparing the transmitted spectra with and without the Er:YAP crystal.

Figure 2 shows the pump absorption spectra of the Er:YAP crystal at 290 K and 77 K. It should be noted that the Er:YAP crystal exhibits an anisotropic structure, such that the measured absorption spectrum is actually the averaged result of polarized absorption along the *a* and *c*-axes of the crystal. At 290 K, the absorption spectrum covered a wide band from 960–1020 nm, and the absorption coefficient corresponding to LD pumping at 976 nm was

1.5 cm^{-1}. When the crystal was cryogenically cooled to 77 K, the absorption spectrum narrowed from 960 nm to less than 1000 nm, and the absorption coefficient at 976 nm decreased to 0.5 cm^{-1}. The changes in the spectral shape and overall reduction in the absorption coefficient at 77 K can be attributed to the influence of the temperature-dependent Boltzmann factor. This result indicates that a higher incident pump power is necessary to achieve a watt-level laser output due to the decreased absorption coefficient at low temperatures.

Thereafter, the crystal was excited by a quasi-CW modulated 976-nm LD with a 100-μs pulse width at different cooling temperatures from 77–290 K. Two high-speed photodetectors working at 1.5 μm (PDA20H-EC, THORLABS) and 3 μm (PVI-4TE-4-1×1, VIGO SYSTEM) were used to detect the fluorescence decays from $^4I_{13/2}$ and $^4I_{11/2}$ multiplets, respectively. The fluorescence lifetimes were fitted from the fluorescence decays using a single exponential decay function. We found that the fluorescence lifetime of the $^4I_{11/2}$ multiplet gradually decreased from 1.34 ms to 0.94 ms; whereas, the lifetime of the $^4I_{13/2}$ multiplet increased from 4.61 ms to 6.27 ms when the cooling temperature was increased from 77 K to 290 K, as shown in Fig. 3. For the crystal, the number of phonons decreases as the cooling temperature decreases, thus resulting in weak multi-phonon coupling. Therefore, the lifetime of the $^4I_{11/2}$ multiplet was expected to increase slightly at low temperatures. However, the energy gap between the $^4I_{13/2}$ multiplet and the ground state $^4I_{15/2}$ is significantly large, such that the lifetime of the $^4I_{13/2}$ multiplet was not significantly influenced by the non-radiative transition driven by multi-phonon coupling. Moreover, the energy transfer up-conversion from the $^4I_{13/2}$ level was enhanced at a lower cooling temperature, which was especially pronounced for a relatively high-doped crystal [22], thus depopulating the $^4I_{13/2}$ multiplet and resulting in a decreased fluorescence lifetime. In terms of the 3-μm laser transition from the $^4I_{11/2}$ level to the $^4I_{13/2}$ level (see inset of Fig. 3), the low operating temperature is beneficial for population inversion and hence laser generation.

Laser experiments on the Er:YAP crystal under cryogenic cooling conditions were conducted using the setup shown in Fig. 4. A 976-nm fiber-coupled and wavelength-stabilized LD (K976AAHRN-27.00WN0N-10522F10ENA, BTW) was used as the pump source, the fiber of which had a core diameter of 105 μm and numerical aperture of 0.22. With a 4:15 telescope system, the pump light was imaged into the crystal with a waist diameter of ~390 μm. A plane input mirror (IM, high transmission at 960–980 nm, and high reflectivity at 2.6–3 μm) and an additional sapphire plate (AR coated at 2.9 μm) were used as cryostat windows. To optimize the laser performance, three output couplers (OCs) with

transmissions of T = 1%, T = 2.5%, and T = 5% were used. With this arrangement, the total cavity length was measured to be 25 mm. A bandpass filter was used to block residual pump light from the laser output.

At 290 K, the single-pass absorption coefficient of the Er:YAP crystal was re-measured using the wavelength-stabilized 976 nm LD. The absorption value of 71% was nearly the same as the above measurement result in Fig. 2, thus confirming the accuracy of the measurement using the setup shown in Fig. 1. Therefore at 77 K, we used the measured single-pass absorption coefficient (0.5 cm^{-1}) to evaluate the absorbed pump power (i.e., 33% of the incident pump power). This evaluation is reasonable because the ground-state bleaching effect can be neglected for highly Er-doped lasers, as demonstrated in our previous study [8]. The output power as a function of the absorbed pump power for the three OCs at 77 K is shown in Fig. 5. With T_{OC} = 1%, the maximum output power was 0.4 W at an absorbed pump power of 7.3 W, corresponding to an average slope efficiency ($\eta_{avg.}$) of 8.3%. As the T_{OC} increased, the output power and slope efficiency of the Er:YAP laser increased, and reached maximum values of 1.2 W and 20%, respectively, at a T_{OC} of 2.5%. The power fluctuation of the Er:YAP laser was monitored to be less than 5% within one hour. It should be noted that we significantly improved the slope efficiency and scaled up the output power by two orders of magnitude when compared with the results reported in [19]. These improvements can be attributed to the use of a relatively highly doped Er:YAP crystal, which enables a larger quantum efficiency due to the enhanced energy transfer up-conversion at a high doping concentration [24]. Note that the further scaling of the output to multi-watt power levels can be realized. However, it is limited by the available absorbed pump power due to the low absorption coefficient at 77 K, thus indicating that using a longer crystal or shifting the pump laser spectrum to a shorter wavelength (i.e., ~960 nm) is a potential solution for future studies.

Despite the optimized laser slope efficiency, the 20% average slope efficiency in the current experiment was lower than our previous results obtained at room temperature [8]. We attribute the reduction in slope efficiency to the increase in cavity loss. Based on the output characteristics shown in Fig. 5, the internal cavity loss was fitted to be ~3.5% according to a Caird analysis [25]. However, the cavity loss was less than 0.5% at room temperature in our previous study [8]. Although the current cavity length was increased when compared with our previous arrangement [8], the length exposed to air was still very short (~5 mm), such that the increase in cavity loss may not be due to vapor absorption. Therefore, we attributed the increased internal loss to the intracavity AR window. Despite the high

transmittance (T > 99.7%) of the AR window, the sapphire-based substrate may not be cut exactly along the *c*-axis, which introduces depolarization loss into the laser cavity, hence resulting in a reduction in the slope efficiency.

The laser spectrum was measured using another optical spectrum analyzer (771B-MIR, Bristol Instruments) with T_{OC} = 2.5%, as it allowed for the optimal laser performance among the three OCs. Figure 6 shows typical Er:YAP laser spectra measured at 77 K at different output powers. The laser spectrum exhibited two peaks at 2723 nm and 2740 nm when the output power was less than 0.1 W, and shifted to 2798 nm with a linewidth of approximately 1.5 nm when the output power was higher than 0.7 W, due to the reabsorption effect from the excited state $^4I_{13/2}$ [8,10]. At watt-level output power, the cryogenic Er:YAP laser emitted at 2798 nm instead of 2920 nm as in the case of room-temperature Er:YAP laser [8]. This can also be explained by the lower reabsorption loss owing to the decreased lifetime of the $^4I_{13/2}$ multiplet (see Fig. 3), as well as the change in the Boltzmann distribution of the Stark levels at low temperatures.

In conclusion, we have demonstrated the spectroscopic and laser properties of a highly doped Er:YAP crystal at cryogenic temperatures. At 77 K, the fluorescence lifetime of the $^4I_{11/2}$ multiplet increased to 1.34 ms, and the lifetime of the $^4I_{13/2}$ multiplet decreased to 4.61 ms, which suggests that low temperatures are beneficial for 3-μm laser generation. In the laser experiment, an output power of 1.2 W was achieved at 2798 nm, with a slope efficiency of 20%. This is the first watt-level Er:YAP laser that operates at cryogenic temperatures. The power and efficiency limits are primarily due to the additional depolarization loss introduced by the intracavity window, which is based on an optically anisotropic substrate. In future research, further improvements in the laser performance can be realized with an appropriately-designed AR window and a longer crystal to absorb a greater fraction of the incident pump power.

Acknowledgments

This work was supported by the JAEA Nuclear Energy S&T and Human Resource Development Project (JPJA P21P21465814), the Japan Society for the Promotion of Science (18H01204), and JST, the establishment of university fellowships towards the creation of science technology innovation (JPMJFS2136).

References

1) F. J. Hernandez, J. T. Brice, C. M. Leavitt, T. Liang, P. L. Raston, G. A. Pino, and G. E. Douberly, The J. Chem. Phys. 143, 164304 (2015).
2) B. M. Walsh, H. R. Lee, and N. P. Barnes, J. Lumin. 169, 400 (2016).
3) K. Karki, S. D. Subedi, D. Martyshkin, V. V. Fedorov, and S. Mirov, Proc. SPIE 11259, 78 (2020).
4) A. V. Pushkin, E. A. Migal, H. Uehara, K. Goya, S. Tokita, M. P. Frolov, Y. V. Korostelin, V. I. Kozlovsky, Y. K. Skasyrsky, and F. V. Potemkin, Opt. Lett. 43, 5941 (2018).
5) E. Li, H. Uehara, W. Yao, S. Tokita, F. Potemkin, and R. Yasuhara, Opt. Express 29, 44118 (2021).
6) V. Fortin, F. Jobin, M. Larose, M. Bernier, and R. Vallée, Opt. Lett. 44, 491 (2019).
7) K. L. Vodopyanov, J. Opt. Soc. Am. B 10(9), 1723 (1993).
8) W. Yao, H. Uehara, H. Kawase, H. Chen, and R. Yasuhara, Opt. Express 28, 19000 (2020).
9) T. Sanamyan, M. Kanskar, Y. Xiao, D. Kedlaya, and M. Dubinskii, Opt. Express 19, A1082 (2011).
10) W. Yao, H. Uehara, S. Tokita, H. Chen, D. Konishi, M. Murakami, and R. Yasuhara, Appl. Phys. Express 14, 012001 (2020).
11) H. Uehara, D. Konishi, K. Goya, R. Sahara, M. Murakami, and S. Tokita, Opt. Lett. 44, 4777 (2019).
12) Y. O. Aydin, V. Fortin, R. Vallée, and M. Bernier, Opt. Lett. 43, 4542 (2018).
13) T. Sanamyan, J. W. Evans, and S. A. McDaniel, Opt. Express 25, 16452 (2017).
14) W. Yao, E. Li, H. Uehara, and R. Yasuhara, Opt. Express 29, 24606 (2021).
15) J. I. Mackenzie, N. Ter-Gabrielyan, and Y.-F. Chen, Appl. Phys. B 127, 49 (2021).
16) T. Sanamyan, J. Simmons, and M. Dubinskii, Laser Phys. Lett. 7, 569 (2010).
17) Z. D. Fleischman and T. Sanamyan, Opt. Mater. Express 6, 3109 (2016).
18) H. Kawase and R. Yasuhara, Opt. Express 27, 12213 (2019).
19) R. Svejkar, J. Sulc, M. Nemec, H. Jelínkova, K. Nejezchleb, and M. Cech, in: Solid State Lasers XXVII: Technology and Devices, 10511 (2018).
20) C. Quan, D. Sun, J. Luo, H. Zhang, Z. Fang, X. Zhao, L. Hu, M. Cheng, Q. Zhang, and S. Yin, Opt. Express 26, 28421 (2018).
21) C. Quan, D. Sun, H. Zhang, J. Luo, L. Hu, Z. Han, Y. Qiao, K. Dong, Y. Chen, M. Cheng, J. Lumin. 251, 119122 (2022).
22) H. Uehara, S. Tokita, J. Kawanaka, D. Konishi, M. Murakami, S. Shimizu, and R. Yasuhara, Opt. Express 26, 3497 (2018).
23) V. A. Antonov, P. A. Arsenev, K. E. Kienert, and A. V. Potemkin, Phys. Status Solidi A 19, 289 (1973).
24) T. Jensen, A. Diening, G. Huber, and B. H. T. Chai, Opt. Lett. 21, 585 (1996).
25) J. A. Caird, S. A. Payne, P. Staber, A. Ramponi, L. Chase, and W. F. Krupke, IEEE J. Quantum Electron. 24, 1077 (1988).

Figure Captions

Fig. 1. Experimental setup of spectroscopic measurement (SC: super-continuum light source; OSA: optical spectrum analyzer).

Fig. 2. Comparison of the Er:YAP absorption spectra at different temperatures.

Fig. 3. Fluorescence lifetimes of (a) $^4I_{13/2}$ and (b) $^4I_{11/2}$ multiplets at different cooling temperatures. Inset: brief energy diagram of Er:YAP at 77 K (ETU: energy transfer up-conversion; NR: nonradiative relaxation) [23].

Fig. 4. Experimental setup of cryogenic Er:YAP laser. LD: laser diode; IM: input mirror; OC: output coupler.

Fig. 5. Laser output power with different T_{OC} values at the liquid nitrogen cooling temperature.

Fig. 6. Typical laser spectra measured at different output powers.

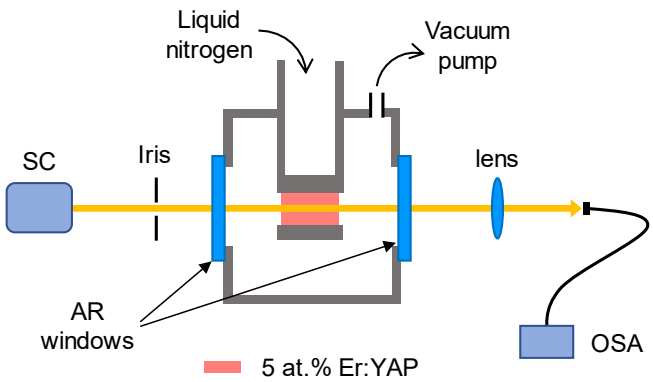

Fig. 1.

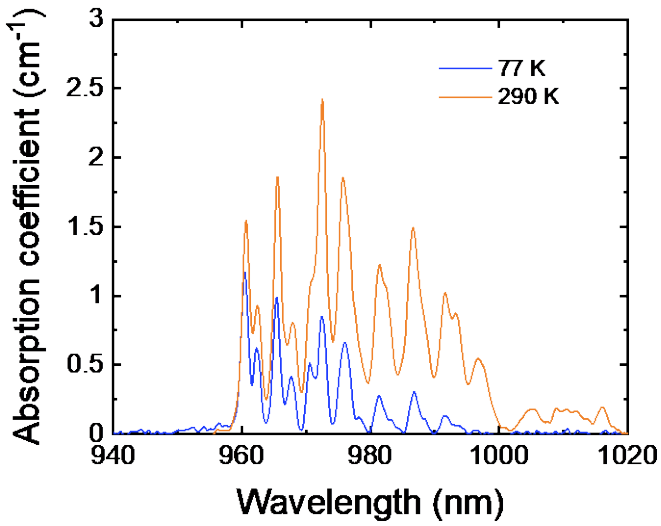

Fig. 2.

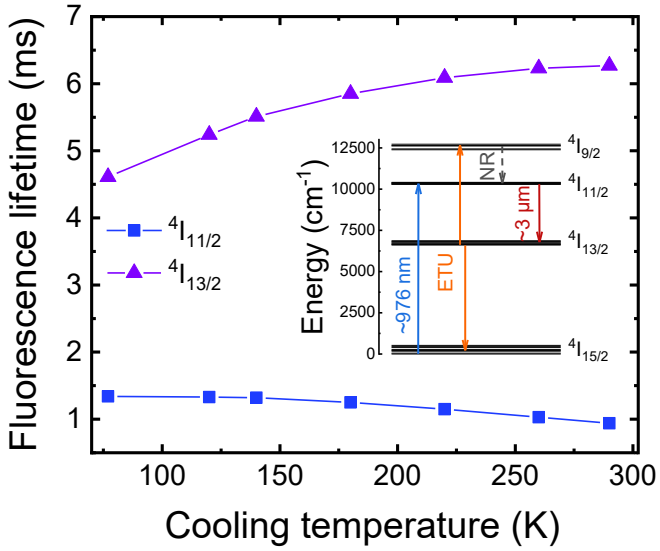

Fig. 3.

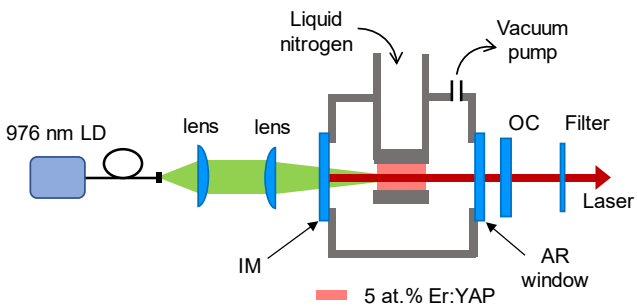

Fig. 4.

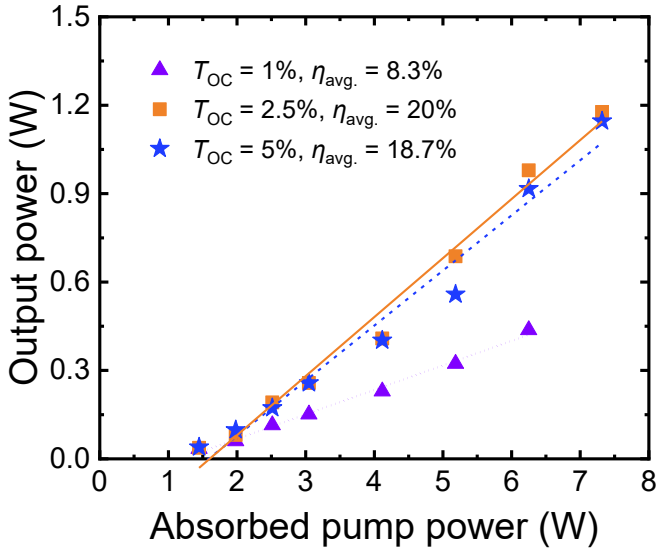
1.5
1.2
0.9
0.6
0.3
0.0
0
1
2
3
4
5
6
7
8
Output power (W)
Absorbed pump power (W)
T_{OC} = 1%, $\eta_{avg.}$ = 8.3%
T_{OC} = 2.5%, $\eta_{avg.}$ = 20%
T_{OC} = 5%, $\eta_{avg.}$ = 18.7%

Fig. 5.

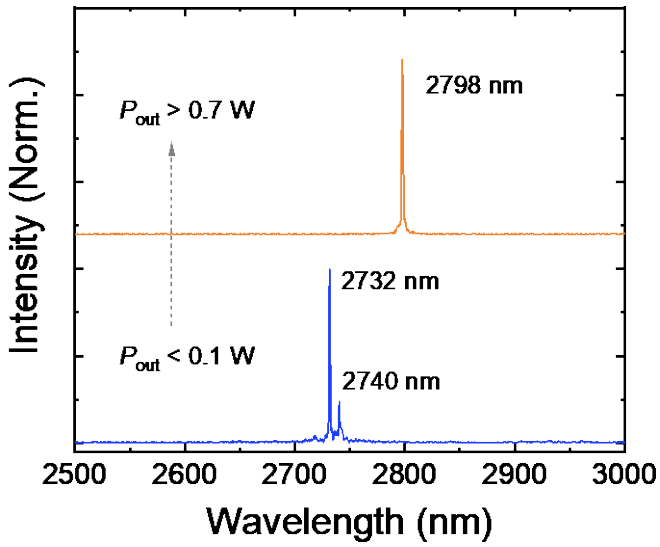
Intensity (Norm.)
Wavelength (nm)
2500
2600
2700
2800
2900
3000
P_{out} > 0.7 W
2798 nm
2732 nm
2740 nm
P_{out} < 0.1 W

Fig. 6.